K^--NUCLEUS POTENTIALS CONSISTENT WITH KAONIC ATOMS*

A. Cieplý[a], E. Friedman[b], A. Gal[b] and J. Mareš[a]

[a]Nuclear Physics Institute, 25068 Řež, Czech Republic
[b]Racah Institute of Physics, The Hebrew University
Jerusalem 91904, Israel

(Received February 5, 2004)

Various models of the K^- nucleus potential have been compared and tested in fits to kaonic atom data. The calculations give basically two vastly different predictions for the depth of the K^- optical potential at the nuclear density. The study of the $(K^-_{\rm stop}, \pi)$ reaction could help to distinguish between K^- optical potentials as the Λ-hypernuclear formation rates are sensitive to the details of the initial-state K^- wave function.

PACS numbers: 24.10.Ht, 36.10.Gv

1. Introduction

In the last decade, we witness an increased interest in exploring the modifications of the K^- mass and interactions in the nuclear medium. The problem is closely related to the question of a possible realization of kaon condensation in neutron stars [1] as well as with the enhanced production of K^- mesons observed in subthreshold and near-threshold heavy ion collisions [2]. Consequently, any direct information on the K^- nucleus interaction (even at ordinary nuclear density and zero temperature) is extremely valuable. In this respect, kaonic atoms represent a unique laboratory for studying strong interactions and nuclear medium effects of antikaons at zero kinetic energy [3]. This contribution is concerned with our recent calculations of the K^- atoms [4,5]. Existing calculations, describing kaonic data reasonably well, basically give two vastly different predictions for the depth of the K^- nucleus potential at nuclear matter density. On one hand, there are phenomenological density dependent (DD) optical potential fits [4,6], and the relativistic mean field (RMF) model [4] which produce a very deep attractive potential

* Presented by J. Mareš at the XXVIII Mazurian Lakes School of Physics, Krzyże, Poland, August 31–September 7, 2003.

($-\mathrm{Re}\ V_{\mathrm{opt}}(\rho_0) \approx$ 150–200 MeV). In contrast, the chirally inspired models of the $\bar{K}N$ interaction [5,7-10], predict much shallower potential ($-\mathrm{Re}\ V_{\mathrm{opt}}(\rho_0) =$ 50–60 MeV). Therefore, one needs different physical data input in order to discriminate between various K^- optical potentials. If the K^- nuclear potential is as strongly attractive as the DD and RMF approaches predict, then deeply bound kaonic nuclei could exist [11]. Of course, the observation of these deeply bound kaonic nuclear states would then give direct information on the K^- optical potential in the nuclear medium.

We have proposed [5] to study the $(K^-_{\mathrm{stop}}, \pi)$ reaction into specific Λ-hypernuclear states. We have found that the hypernuclear formation probabilities are strongly sensitive to the form of the K^- wave function and consequently to the underlying K^- optical potential.

In the next section, we briefly review the models which we have confronted with the entire set of atomic data. In Section 3, we discuss the results of our study of the Λ-hypernuclear production in the $(K^-_{\mathrm{stop}}, \pi)$ reaction. Conclusions are drawn in Section 4.

2. Optical potentials for kaonic atoms

The interaction of K^- with the nucleus in a kaonic atom is commonly described by the Klein–Gordon equation [3]

$$\left[\nabla^2 - 2\mu(B + V_{\mathrm{opt}} + V_{\mathrm{c}}) + (V_{\mathrm{c}} + B)^2\right]\psi = 0 \quad (\hbar = c = 1)\,. \tag{1}$$

Here, μ is the K^- nucleus reduced mass, B is the complex binding energy, V_{opt} denotes the K^- nucleus optical potential due to the strong interaction, and V_{c} is the finite size Coulomb interaction including vacuum polarization terms. The models used for the construction of the K^- optical potential V are briefly introduced in the following subsection.

2.1. Models

2.1.1. Density dependent (DD) potential

The phenomenological analysis of kaonic atoms was performed using the DD potential of the form [6]

$$2\mu V_{\mathrm{opt}}(r) = -4\pi\left(1 + \frac{\mu}{M}\right) b(\rho)\rho(r)\,, \quad b(\rho) = b_0 + B_0\left(\frac{\rho(r)}{\rho_0}\right)^{\alpha}\,. \tag{2}$$

Here, M is the nucleon mass, $\rho(r)$ is the nuclear density distribution, and $\rho_0 =$0.17 fm^{-3}. The parameters α, b_0 and B_0 are determined by fitting the atomic data. For b_0 equal to minus the free K^-N scattering length, the low density limit is satisfied: The potential is repulsive at low densities, reflecting

the presence of the subthreshold $\Lambda(1405)$ resonance. Scattering through this resonance, which is considered to be an unstable K^-p bound state, gives rise to this repulsion. As any fit to the atomic data yields $\mathrm{Re}(b_0 + B_0) > 0$, the DD potential becomes attractive in the nuclear interior. The transition from the repulsion to attraction occurs near $\rho/\rho_0 = 0.15$. The introduction of the density dependence (2) substantially improved former fits done using an ordinary $t_{\mathrm{eff}}\rho$ potential.

2.1.2. Hybrid (RMF+DD) potential

In the derivation of the K^- optical potential within the relativistic mean field approach we used the standard Lagrangian for the nucleons with the linear [12] as well as nonlinear parametrizations [13]. The kaonic sector was incorporated into the model by using the Lagrangian density

$$\begin{aligned}\mathcal{L}_K \;=\; & \partial_\mu \bar{K}\partial^\mu K - m_K^2 \bar{K}K - g_{\sigma K} m_K \bar{K}K\sigma \\ & -ig_{\omega K}(\bar{K}\partial_\mu K\omega^\mu - K\partial_\mu \bar{K}\omega^\mu) + (g_{\omega K}\omega_\mu)^2 \bar{K}K\,, \end{aligned} \tag{3}$$

describing the interaction of the (anti)kaon field K ($\bar{K}$) with the scalar (σ) and the vector (ω) isoscalar fields. The relevant equation of motion for K^- in a $N = Z$ nucleus is the Klein–Gordon equation with the real part of the optical potential given at threshold by

$$\mathrm{Re}\; V_{\mathrm{opt}} = \frac{m_K}{\mu}\left(\frac{1}{2}S - V - \frac{V^2}{2m_K}\right)\,, \tag{4}$$

where $S = g_{\sigma K}\sigma$ and $V = g_{\omega K}\omega_0$ in terms of the mean isoscalar fields. In the case of antikaons, each term on the r.h.s. of Eq. (4) gives rise to attraction. Consequently, it is impossible to satisfy the low density limit which requires repulsive $\mathrm{Re}\; V_{\mathrm{opt}}$ for $\rho \to 0$. The existence of the $\Lambda(1405)$ thus poses a difficulty for the RMF model. It is clear that a mean field approach cannot be applied reliably in the low density region where the K^- interaction with the nucleus is affected by the $\Lambda(1405)$. Therefore, we combined the RMF and the phenomenological DD approaches into a hybrid model [4]. We applied the RMF description in the nuclear interior, where a mean field approach is well justified and where the effect of the $\Lambda(1405)$ resonance may be neglected. In the low density region where the K^- interaction is affected by the $\Lambda(1405)$, we adopted the DD potential from the previous subsection. The sensitivity to the chosen radius R_{M}, where the two forms were matched, was found to be small. The corresponding density $\rho(R_{\mathrm{M}})$ ($\rho(R_{\mathrm{M}}) \approx \rho_0/2$) was significantly high to justify the RMF approach and, at the same time, sufficiently low so that the atomic data were still sensitive to the RMF form.

Fitting the K^- atomic data, the coupling constant $g_{\omega K}$ was kept fixed (by quark model or SU(3) relation), whereas $g_{\sigma K}$ was varied together with the parameters of the DD potential. For the imaginary potential, the pure phenomenological DD form was used.

2.1.3. Chirally motivated model

We applied the chirally motivated model [7,8] for the $\bar{K}N$ scattering and reactions near threshold. In this approach, the K^-p resonance $\Lambda(1405)$ is generated dynamically by solving coupled Lippmann–Schwinger equations for the meson–baryon t-matrix in terms of the input chiral potentials. The use of a nonrelativistic formalism is justified for energies close to the $\bar{K}N$ threshold, which is the case of our study. The six coupled channels included in our model are: K^-p, $\bar{K}^0n$, $\pi^0\Lambda$, $\pi^+\Sigma^-$, $\pi^0\Sigma^0$ and $\pi^-\Sigma^+$. In the coupled channel calculation of the in-medium t matrix, the density dependence of the K^- optical potential can be traced to the propagation of the $\Lambda(1405)$ in the nuclear medium. The transition from a repulsive $t(\rho = 0)$ to an attractive $t(\rho)$ in the nuclear medium is primarily due to Pauli blocking of the intermediate nucleon [14]. Later, Lutz emphasized the relevance of the self consistent treatment of kaon selfenergy [15] and Ramos and Oset included pion, nucleon and hyperon selfenergies, as well [9].

The chirally motivated coupled channel approach to the $\bar{K}N$ interaction was successful in reproducing the low energy K^-p data [7,8]. By introducing selfconsistency it became possible to obtain barely acceptable fits to the kaonic atom data [9]. The fits have been significantly improved by introducing empirical modifications of the interaction [10], but at the cost of losing direct contact with the underlying $\bar{K}N$ interaction model.

In our recent work [5], we addressed the problem by requiring *simultaneous* fits to atomic and K^-p data within the chirally motivated coupled channel approach. We included K^- and N selfenergies in our calculations. The density dependent $\bar{K}N$ interaction was calculated selfconsistently: the K^- optical potential constructed from the elementary $\bar{K}N$ amplitude entered the in-medium propagator through kaon selfenergy. The model was applied in χ^2 fits to K^- atomic data and to representative low energy K^-p data (see Ref. [5] for details).

2.2. Results

We fitted 65 kaonic atom data points. In Table I, the results for the DD, RMF and chiral models are summarized. They are represented by the values of χ^2 per data point and the depths of the optical potentials at $\rho_0 = 0.17$ fm^{-3} (real V_{R} and imaginary V_{I}). The details can be found in Refs. [5,6].

Table I clearly demonstrates that there exist different models of the K^- nucleus interaction consistent with kaonic atom data, which predict considerably different potential depths in the nuclear interior.

TABLE I

Optical potentials fitting K^- atomic data (see text for details).

model	DD	RMF	Chiral
χ^2/N	1.28	1.40	2.24
$V_{\rm R}$(MeV)	−190	−185	−55
$V_{\rm I}$(MeV)	−55	−60	−60

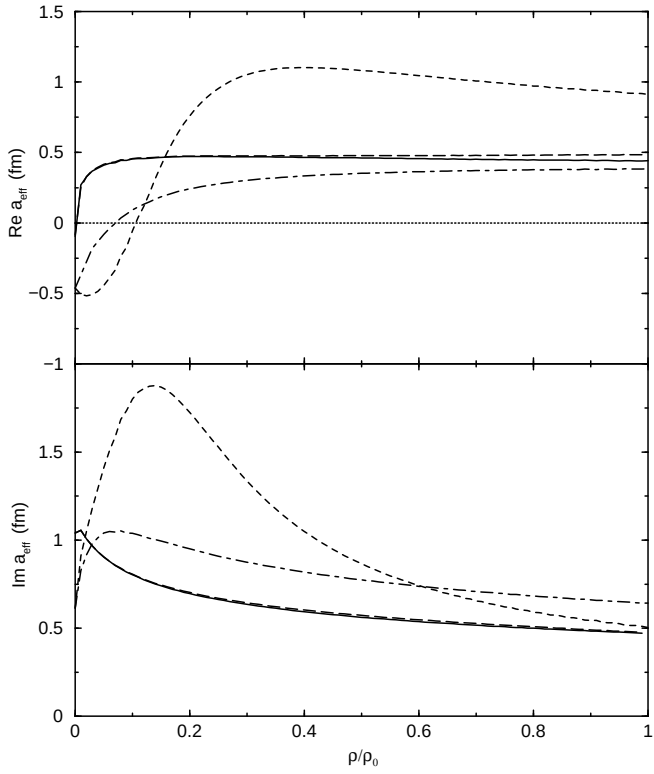

Fig. 1. Real (top) and imaginary (bottom) parts of $a_{\rm eff}$ as function of density ρ/ρ_0, calculated in the 'no Π' (short-dashed line), '$\Pi_{\bar K}$' (dot-dashed line) and '$\Pi_{\bar K}+\Pi_N$' (solid line) regimes. The long-dashed line correspond to the case when the pion and hyperon selfenergies were taken into account as well. (See text for details.)

It is to be noted, that the good agreement of the chiral model with atomic and low-energy K^-p data at the same time was achieved by only minor modifications of the original parameters. While including K^- and N selfenergies in our chiral model appeared crucial (the description of the atomic characteristics improved dramatically from the original $\chi^2/N = 16.5$ to $\chi^2/N = 2.24$), the pion and hyperon selfenergies to the propagator in non-kaonic channels were found to have only marginal effect. This is demonstrated in Fig. 1 where the isospin averaged $\bar{K}N$ threshold scattering amplitude is shown as function of density for the following cases:

(a) no medium effects except Pauli blocking are included ('no Π'),

(b) the selfconsistent calculation including the kaon selfenergy ($\Pi_{\bar{K}}$),

(c) the selfconsistent calculation including the kaon and nucleon selfenergies ($\Pi_{\bar{K}} + \Pi_N$),

(d) plus including the pion and hyperon selfenergies.

Taking the kaon and nucleon selfenergies into account generally leads to a weaker density dependence of the threshold amplitude.

We should stress here that our chiral model gives superior description of kaonic atoms when compared with other chiral models [9,10]. Nevertheless, the phenomenological and the hybrid RMF+DD model give even better χ^2/N as shown in Table I.

The main lesson from the study presented in this section is that the kaonic atom data themselves are not sufficient to determine unambiguously the depth of the K^- optical potential.

3. (K^-, π) reactions as a test of the K^- optical potential

Models of the K^- nucleus interaction at threshold can be tested in (K^-, π) reactions to specific Λ-hypernuclear states. We have calculated the hypernuclear formation rates within the DWIA approach (described in Ref. [16]) with the aim to study their sensitivity to the initial-state kaon wave function and consequently to the underlying K^- optical potential. For the sake of illustration, we present here the results for the K^- capture-at-rest reactions on ^{12}C:

$$K^- + {}^{12}\mathrm{C} \longrightarrow \pi^- + {}^{12}_{\Lambda}\mathrm{C}\,, \qquad K^- + {}^{12}\mathrm{C} \longrightarrow \pi^0 + {}^{12}_{\Lambda}\mathrm{B}\,. \tag{5}$$

While the first process has been a standard tool in hypernuclear spectroscopy, the second has been studied in experiment just recently [18]. Results of our calculations for the K^- optical potentials presented in Section 2 are summarized in Table II.

It is clear from Table II that the deeper the potential is involved in the DWIA calculations, the lower production rate is obtained. This is due to the sensitivity of the distorted-wave integrals to the node structure of the kaon wave function, which is quite different for deep and for shallow potentials. The predicted rates differ by more than a factor of 3 for the considered potentials. Unfortunately, these rates are still much lower than the experimental values even though the new data from the E907 BNL experiment [18] are significantly closer to the calculated values. This discrepancy could stem from uncertainties in the calculation due to the pion distortion effects and/or due to the adopted value of in-medium $K^-N \longrightarrow \pi\Lambda$ capture at rest branching ratio.

TABLE II

Calculated capture rates on ^{12}C per stopped K^- (in units of 10^{-3}) to the summed $p_N \rightarrow s_\Lambda$ 1^- excitations in $^{12}_{\Lambda}$C and $^{12}_{\Lambda}$B, for the K^- optical potentials of Table I. Experimental values are shown for comparison. (The ratio of the rates $^{12}_{\Lambda}\mathrm{C}/^{12}_{\Lambda}\mathrm{B} \approx 2$ by charge independence.)

final $^{A}_{\Lambda}$Z	chiral	DD	exp [17]	exp [18]
$^{12}_{\Lambda}$C	0.231	0.063	0.98 ± 0.12	—
$^{12}_{\Lambda}$B	0.119	0.032	—	0.28 ± 0.08

4. Conclusions

We have demonstrated that current calculations of kaonic atoms essentially give two different predictions for the depth of the K^- nucleus potential at nuclear density. The phenomenological DD and RMF approaches produce deeply attractive potentials, whereas the chirally inspired models predict potentials about 3 times shallower.

The calculated hypernuclear production rates in the $(K^-_{\mathrm{stop}}, \pi)$ reaction exhibit strong dependence on the initial-state kaon wave function and thus on the adopted K^- optical potential. Once ambiguities remaining in the calculation of the capture rates are settled, one should be able to distinguish among existing K^- optical potentials. More experimental data on the $(K^-_{\mathrm{stop}}, \pi)$ hypernuclear production are welcome, as well.

This work was partly supported by the GA AVCR grant IAA1048305 and by the Israel Science Foundation grant No. 131/01.

REFERENCES

[1] H. Heiselberg, H. Hjorth-Jensen, *Phys. Rep.* **328**, 237 (2000).

[2] F. Laue *et al.*, *Phys. Rev. Lett.* **82**, 1640 (1999).

[3] C.J. Batty, E. Friedman, A. Gal, *Phys. Rep.* **287**, 385 (1997).

[4] E. Friedman, A. Gal, J. Mares, A. Cieply, *Phys. Rev.* **C60**, 024314 (1999).

[5] A. Cieply, E. Friedman, A. Gal, J. Mares, *Nucl. Phys.* **A696**, 173 (2001).

[6] E. Friedman, A. Gal, C.J. Batty, *Phys. Lett.* **B308**, 6 (1993); *Nucl. Phys.* **A579**, 518 (1994).

[7] N. Kaiser, P.B. Siegel, W. Weise, *Nucl. Phys.* **A594**, 325 (1995).

[8] T. Waas, N. Kaiser, W. Weise, *Phys. Lett.* **B365**, 12 (1996); **379**, 34 (1996).

[9] A. Ramos, E. Oset, *Nucl. Phys.* **A671**, 481 (2000).

[10] A. Baca, C. García-Recio, J. Nieves, *Nucl. Phys.* **A673**, 335 (2000).

[11] Y.Akaishi, T. Yamazaki, *Phys. Rev.* **C65**, 044005 (2002); T. Kishimoto, *Phys. Rev. Lett.* **83**, 4701 (1999).

[12] C.J. Horowitz, B.D. Serot, *Nucl. Phys.* **A368**, 503 (1981).

[13] P.-G. Reinhard, M. Rufa, J. Maruhn, W. Greiner, J. Friedrich, *Z. Phys.* **A323**, 13 (1986).

[14] V. Koch, *Phys. Lett.* **B337**, 1 (1994).

[15] M. Lutz, *Phys. Lett.* **B426**, 12 (1998).

[16] A. Gal, E. Klieb, *Phys. Rev.* **C34**, 956 (1986).

[17] H. Tamura, R.S. Hayano, H. Outa, T. Yamazaki, *Progr. Theor. Phys. Suppl.* **117**, 1 (1994).

[18] E. Hungerford, private communication; M.W. Ahmed *et al.*, *Phys. Rev.* **C68**, 064004 (2003).